

# Spin squeezing with short-range spin-exchange interactions

Michael A. Perlin,<sup>1,2,\*</sup> Chunlei Qu,<sup>3,†</sup> and Ana Maria Rey<sup>1,2</sup>

<sup>1</sup>*JILA, National Institute of Standards and Technology and University of Colorado, 440 UCB, Boulder, Colorado 80309, USA*

<sup>2</sup>*Center for Theory of Quantum Matter, University of Colorado, Boulder, CO, 80309, USA*

<sup>3</sup>*Department of Physics and Center for Quantum Science and Engineering, Stevens Institute of Technology, 1 Castle Point Terrace, Hoboken, NJ 07030, USA*

(Dated: June 14, 2022)

We investigate many-body spin squeezing dynamics in an XXZ model with interactions that fall off with distance  $r$  as  $1/r^\alpha$  in  $D = 2$  and 3 spatial dimensions. In stark contrast to the Ising model, we find a broad parameter regime where spin squeezing comparable to the infinite-range  $\alpha = 0$  limit is achievable even when interactions are short-ranged,  $\alpha > D$ . A region of “collective” behavior in which optimal squeezing grows with system size extends all the way to the  $\alpha \rightarrow \infty$  limit of nearest-neighbor interactions, where achievable squeezing is primarily limited by the coherence time of a system. We identify the boundary between collective and Ising-limited squeezing behaviors with a dynamical phase transition between regions of parametrically distinct entanglement growth. Our predictions, made using the discrete truncated Wigner approximation (DTWA), are testable in a variety of experimental cold atomic, molecular, and optical platforms.

*Introduction* – Quantum technologies receive an enormous amount of attention for their potential to push beyond classical limits on physically achievable tasks. In order to be useful, however, these technologies must demonstrate a practical advantage over their classical counterparts. While most public attention has focused on a quantum advantage in the realm of computing, the quantum metrology community has made tremendous progress in developing strategies and platforms for surpassing classical limits on measurement precision [1–4]. A key element in these strategies is the use of entanglement to enhance the capabilities of individual, uncorrelated quantum systems. Spin squeezing is one of the most promising strategies for using entanglement to achieve a quantum advantage in practical sensing applications [5, 6].

The paradigmatic setting for spin squeezing is the *one-axis twisting* (OAT) model [6, 7], which generates spin-squeezed states by use of uniform, infinite-range Ising interactions that do not distinguish between the constituent spins. These uniform interactions can be implemented directly via collisional interactions between delocalized atoms [8–10], as well as indirectly through coupling to collective phonon modes [11, 12] or cavity photons [13–17]. In general, however, the absence of locality in the OAT model poses a major challenge for its implementation in systems with contact or power-law interactions that fall off with distance  $r$  as  $1/r^\alpha$ . While the Ising model with power-law interactions can be shown to achieve an amount of spin squeezing that scales with system size for any  $\alpha < D$  in  $D$  spatial dimensions [18], for  $\alpha \geq D$  the Ising model generates only a small amount of squeezing that is independent of system size, which places severe restrictions on its metrological utility.

Motivated by the intuition (echoed in Refs. [10, 19–23]) that adding spin-exchange interactions to the Ising model should energetically protect collective behavior

reminiscent of the OAT model, in this work we investigate the spin squeezing properties of the power-law XXZ model. Remarkably, we find a broad range of parameters for which the power-law XXZ model nearly saturates the amount of squeezing generated in the infinite-range ( $\alpha = 0$ ) limit. Even when interactions are short-ranged ( $\alpha > D$ ), we observe a large region of “collective” squeezing behavior in which the amount of achievable spin squeezing grows with system size. This region extends through to the  $\alpha \rightarrow \infty$  limit of nearest-neighbor interactions, where squeezing is essentially limited by the coherence time of a system. We identify the transition from collective to Ising-limited squeezing behavior with a dynamical phase transition between regions of parametrically distinct entanglement growth [24, 25]. Our work opens up the prospect of spin squeezing in variety of cold atomic, molecular, and optical (AMO) systems, including ultracold neutral atoms [26, 27], Rydberg atoms [28, 29], electric and magnetic dipolar quantum gasses [30–33], and trapped ions [11, 34].

*Background and theory* – We begin with a brief review of spin squeezing and the OAT model, described by the Ising Hamiltonian

$$H_{\text{OAT}} = \chi \sum_{i,j=1}^N s_{z,i} s_{z,j} = \chi S_z^2, \quad (1)$$

where  $\chi$  is the OAT squeezing strength; the spin- $z$  operator  $s_{z,i} \equiv \sigma_{z,i}/2$  is defined in terms of the Pauli- $z$  operator  $\sigma_{z,i}$  on spin  $i$ ; and  $S_z \equiv \sum_{i=1}^N s_{z,i}$  is a collective spin- $z$  operator. Eigenstates of  $H_{\text{OAT}}$  can be classified by a (nonnegative) total spin  $S \in \{N/2, N/2 - 1, \dots\}$ , and a projection  $m_z \in \{S, S - 1, \dots, -S\}$  of spin onto the  $z$  axis. The manifold of all states with maximal total spin  $S = N/2$  (e.g. spin-polarized states) is known as the *Dicke manifold* [6]. Equivalently, the Dicke manifold consists of all *permutationally symmetric* states that do

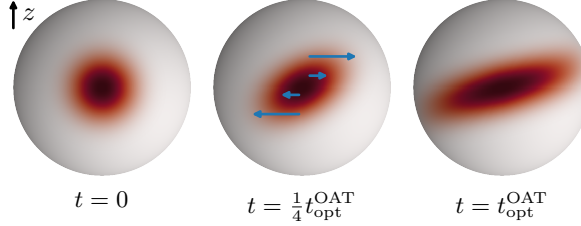


FIG. 1. Representations of the state  $|\psi(t)\rangle$  of  $N = 40$  spins initially polarized along the equator, and evolved under the OAT Hamiltonian for a time  $t$  up to the optimal OAT squeezing time  $\chi t_{\text{opt}}^{\text{OAT}} \sim 1/N^{2/3}$ . Darker colors at a point  $\hat{\mathbf{n}}$  on the sphere correspond to a larger overlap  $Q_{\psi(t)}(\hat{\mathbf{n}}) \equiv |\langle \hat{\mathbf{n}} | \psi(t) \rangle|^2$ , where  $|\hat{\mathbf{n}}\rangle$  is a state in which all spins are polarized along  $\hat{\mathbf{n}}$ .

not distinguish between underlying spins. Similarly to how the state of a single spin can be represented by a point on the Bloch sphere, collective states in the Dicke manifold can be represented by *distributions* on a sphere, whose variances along different directions must satisfy an appropriate set of quantum (Heisenberg) uncertainty relations (see Figure 1). Just as an individual spin- $z$  operator rotates the state of a single spin about the  $z$  axis, the collective operator  $S_z = \sum_{m_z} m_z |m_z\rangle\langle m_z|$  rotates the entire distribution about the  $z$  axis. The OAT Hamiltonian  $\sim S_z^2 = \sum_{m_z} |m_z\rangle\langle m_z| \times m_z S_z$  can therefore be thought of as a rotation about the  $z$  axis at a rate proportional to the spin projection  $m_z$ , i.e. twisting about the  $z$  axis.

Given an initial state polarized along the equator, represented by a Gaussian distribution on the sphere, the net effect of the OAT Hamiltonian is to shear this distribution, resulting in a *squeezed* state with a reduced variance  $(\Delta\phi)^2$  along some axis. This reduced variance allows for an enhanced measurement sensitivity to rotations of the collective spin state along the squeezed axis, at the expense of a reduced sensitivity to rotations about an orthogonal axis. Spin squeezing can be quantified by the maximal gain in angular resolution  $\Delta\phi$  over that achieved by a spin-polarized state [6],

$$\xi^2 \equiv \frac{(\Delta\phi_{\text{min}})^2}{(\Delta\phi_{\text{polarized}})^2} = \min_{\phi} \text{var}(S_{\phi}^{\perp}) \times \frac{N}{|\langle \mathbf{S} \rangle|^2}, \quad (2)$$

where  $\mathbf{S} \equiv (S_x, S_y, S_z)$  is a vector of collective spin operators; the operator  $S_{\phi}^{\perp} \equiv \mathbf{S} \cdot \hat{\mathbf{n}}_{\phi}^{\perp}$  is the projection of  $\mathbf{S}$  onto an axis  $\hat{\mathbf{n}}_{\phi}^{\perp}$  parameterized by an angle  $\phi$  in the plane orthogonal to the mean spin vector  $\langle \mathbf{S} \rangle$ ; and  $\text{var}(\mathcal{O}) \equiv \langle \mathcal{O}^2 \rangle - \langle \mathcal{O} \rangle^2$  denotes the variance of  $\mathcal{O}$ . A spin squeezing parameter  $\xi^2 < 1$  implies the presence of many-body entanglement [24] that enables a sensitivity to rotations beyond that set by classical limits on measurement precision [1]. The OAT model can prepare squeezed states with  $\xi^2 \sim 1/N^{2/3}$ , whereas the fundamental (“Heisenberg”) limit imposed by quantum mechanics is  $\xi^2 \sim 1/N$  [1].

To accommodate for the fact that physical interactions are typically local, the OAT Hamiltonian in Eq. (1) can be modified by the introduction of coefficients  $1/|\mathbf{r}_i - \mathbf{r}_j|^{\alpha}$  in the coupling between spins  $i, j$  at positions  $\mathbf{r}_i, \mathbf{r}_j$ , resulting in the power-law Ising model. The introduction of non-uniform couplings means that the power-law Ising model breaks permutational symmetry, coupling the Dicke manifold of permutationally symmetric states with total spin  $S = N/2$  to asymmetric states with  $S < N/2$ , and thereby invalidating the representation of squeezing dynamics shown in Figure 1. The leakage of population outside the manifold of permutationally symmetric states can be energetically suppressed by the additional introduction of spin-aligning  $\mathbf{s}_i \cdot \mathbf{s}_j$  interactions, where  $\mathbf{s}_i \equiv (s_{x,i}, s_{y,i}, s_{z,i})$  is the spin vector for spin  $i$ . In total, we thus arrive at an XXZ model described by the Hamiltonian

$$H_{\text{XXZ}} = \sum_{i \neq j} \frac{J_{\perp} \mathbf{s}_i \cdot \mathbf{s}_j + (J_z - J_{\perp}) s_{z,i} s_{z,j}}{|\mathbf{r}_i - \mathbf{r}_j|^{\alpha}} \quad (3)$$

where the power-law Ising Hamiltonian is a special case of  $H_{\text{XXZ}}$  with  $J_{\perp} = 0$  and  $J_z = \chi$ . When interactions are uniform,  $\alpha = 0$ , the  $\sum_{i \neq j} \mathbf{s}_i \cdot \mathbf{s}_j \sim \mathbf{S}^2 = S(S+1)$  terms in Eq. (3) are constant within manifolds of definite total spin  $S$ , resulting in an OAT model with  $\chi = J_z - J_{\perp}$ .

When  $J_z - J_{\perp} = 0$ , the XXZ model contains only the spin-aligning  $\mathbf{s}_i \cdot \mathbf{s}_j$  terms, and if interactions are long-ranged,  $\alpha \leq D$ , then the Dicke manifold is gapped away from all orthogonal states by a non-vanishing energy difference  $\Delta_{\text{gap}} \gtrsim |J_{\perp}|$  (see [35]). As a consequence, for any  $\alpha \leq D$  there exists a non-vanishing range of coupling strengths  $J_z \approx J_{\perp}$  for which a perturbative treatment of the anisotropic ZZ terms in Eq. (3) is valid. In this case, the XXZ model becomes precisely the OAT model at first order in perturbation theory, with a squeezing strength  $\chi_{\text{eff}} = h_{\alpha} (J_z - J_{\perp})$ , where  $h_{\alpha}$  is the average of  $1/|\mathbf{r}_i - \mathbf{r}_j|^{\alpha}$  over all  $i \neq j$ . If interactions are short-ranged with  $\alpha > D$ , then generally  $\Delta_{\text{gap}} \rightarrow 0$  in the thermodynamic limit  $N \rightarrow \infty$ , formally invalidating perturbation theory. Nonetheless, the spin-aligning terms of the XXZ model can still enable a non-perturbative emergence of “collective” behavior resembling perturbative, gap-protected OAT. We numerically explore the prospect of spin squeezing with short-ranged interactions in the following section, finding that squeezing comparable to OAT may be possible with a wide range of  $\alpha$  and  $J_z$ , including the  $\alpha \rightarrow \infty$  limit of nearest-neighbor interactions.

*Results* – Whereas the quantum Ising model is exactly solvable [36, 37], the XXZ model in Eq. (3) is not. Furthermore, the exponential growth of Hilbert space limits the scope of exact numerical simulations to small systems of little practical relevance. We therefore investigate the spin squeezing properties of the XXZ model using the discrete truncated Wigner approximation (DTWA)

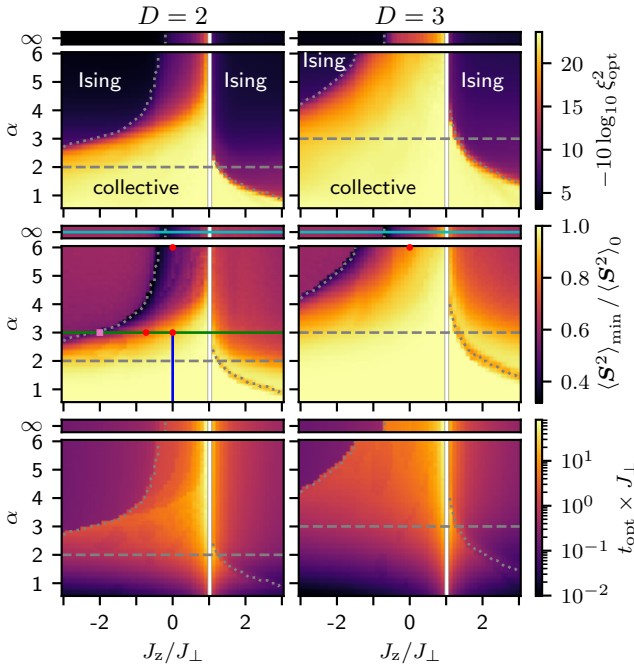


FIG. 2. The optimal squeezing  $\xi_{\text{opt}}^2$  (top), minimal squared spin length  $\langle \mathbf{S}^2 \rangle_{\text{min}}$  (middle), and optimal squeezing time  $t_{\text{opt}}$  (bottom) for  $4096 = 64^2 = 16^3$  spins in  $D = 2$  (left) and  $D = 3$  (right) spatial dimensions. Spins are initially polarized along the equator and evolved under the XXZ Hamiltonian in Eq. (3). Squeezing  $\xi_{\text{opt}}^2$  is shown in decibels, and  $\langle \mathbf{S}^2 \rangle_{\text{min}}$  is normalized to its initial value  $\langle \mathbf{S}^2 \rangle_0 = \frac{N}{2} \left( \frac{N}{2} + 1 \right)$ . Dashed grey lines mark  $\alpha = D$ , and dotted grey lines track local minima of  $\langle \mathbf{S}^2 \rangle_{\text{min}}$ , marking the boundary between regions of collective and Ising-limited squeezing dynamics. Other markers in the middle panels indicate values of  $J_z/J_{\perp}, \alpha, D$  that are currently accessible with neutral atoms [40, 41] (cyan line), Rydberg atoms [28, 29, 42] (red dots), polar molecules [30, 31, 43] (green line), magnetic atoms [32, 33] (pink square), and trapped ions [11] (blue line).

[38] for  $4096 = 64^2 = 16^3$  spins, focusing on the case of two ( $D = 2$ ) and three ( $D = 3$ ) spatial dimensions (see [35] for  $D = 1$ , where our main results are less striking but still hold). DTWA has been shown to accurately capture the behavior of collective spin observables in a variety of settings [38, 39], and we provide additional benchmarking of DTWA for the XXZ model on a  $7 \times 7$  lattice in [35]. Our main results are summarized in Figure 2, in which we explore the squeezing behavior of XXZ model in Eq. (3) around criticality (at  $J_z = J_{\perp}$ ) by varying both  $J_z/J_{\perp}$  and the power-law exponent  $\alpha$ . Specifically, we examine (i) the optimal squeezing parameter  $\xi_{\text{opt}}^2 \equiv \min_t \xi^2(t) = \xi^2(t_{\text{opt}})$ , (ii) the minimal squared spin length throughout squeezing dynamics,  $\langle \mathbf{S}^2 \rangle_{\text{min}} \equiv \min_{t \leq t_{\text{opt}}} \langle \mathbf{S}^2 \rangle(t)$ , and (iii) the optimal squeezing time  $t_{\text{opt}}$ .

First and foremost, Figure 2 confirms the theoretical argument that OAT-limited squeezing should be achievable with any power-law exponent  $\alpha \leq D$  for some non-

vanishing range of of couplings ZZ  $J_z \approx J_{\perp}$ . Surprisingly, this capability persists well beyond the perturbative window with  $|J_z - J_{\perp}| \ll |J_{\perp}|$ , covering all  $J_z < J_{\perp}$  shown in Figure 2 and an increasing range of  $J_z > J_{\perp}$  with decreasing  $\alpha$  for  $\alpha \lesssim D$ . For short range interacting systems at equilibrium, the region  $J_z < J_{\perp}$  corresponds to the easy-plane ( $|J_z| < |J_{\perp}|$ ) and ferromagnetic ( $J_z/J_{\perp} < -1$ ) phases of the XXZ model, whereas  $J_z > J_{\perp}$  corresponds to the anti-ferromagnetic phase. The asymmetry about  $J_z = J_{\perp}$  in Figure 2 therefore suggests an interesting connection between equilibrium physics and far-from-equilibrium dynamical behavior of the XXZ model.

Even more strikingly than the behavior at  $\alpha \leq D$ , Figure 2 shows that squeezing well beyond the Ising limit can still achievable for a wide range of ZZ couplings  $J_z < J_{\perp}$  when interactions are short-ranged,  $\alpha > D$ . Though the attainable amount of squeezing generally decreases with shorter range (increasing  $\alpha$ ) and stronger anisotropy (decreasing  $J_z < J_{\perp}$ ), a region of “collective” squeezing behavior smoothly connected to the OAT limit persists through to the  $\alpha \rightarrow \infty$  limit of nearest-neighbor interactions. This region is related to the  $\frac{2}{3}D \leq \alpha < D$  region of the power-law Ising model ( $J_z/J_{\perp} \rightarrow \pm\infty$ ), in which squeezing falls short of the OAT limit, but still grows with system size [18].

In fact, the transition from collective to Ising-limited squeezing is marked by a discontinuous change in both the minimal squared spin length  $\langle \mathbf{S}^2 \rangle_{\text{min}}$  and the optimal squeezing time  $t_{\text{opt}}$ , signifying the presence of a dynamical phase transition. The dynamical phases in question can be characterized by the behavior of optimal squeezing  $\xi_{\text{opt}}^2$ , which either scales with system size (in the collective phase) or saturates to a constant value (in the Ising-limited phase). We discuss and clarify these points below.

The discontinuity in optimal squeezing time  $t_{\text{opt}}$  at the dynamical phase transition in Figure 2 is the result of a competition between local optima in squeezing over time, shown in Figure 3. Large amounts of spin squeezing are generated by collective dynamics near the critical point of the XXZ model at  $J_z = J_{\perp}$ . The amount of squeezing generated by collective dynamics falls off away from the critical point, until it finally drops below an “Ising” squeezing peak that is generated at much short times, resulting in a discontinuous change in the time at which squeezing is optimal. The discontinuous change in the optimal squeezing time is in turn responsible for the sudden change in the minimal squared spin length  $\langle \mathbf{S}^2 \rangle_{\text{min}}$ , which has less time to decay in the Ising-limited regime. We note that the precise mechanism for collective dynamics far from the critical point at  $J_z = J_{\perp}$  is not obvious, especially given the appreciable decay of the squared spin length  $\langle \mathbf{S}^2 \rangle$  close to the collective-to-Ising transition (see middle panels of Figure 2, and the bottom panel in Figure 3). The mechanism underlying collective dynamics

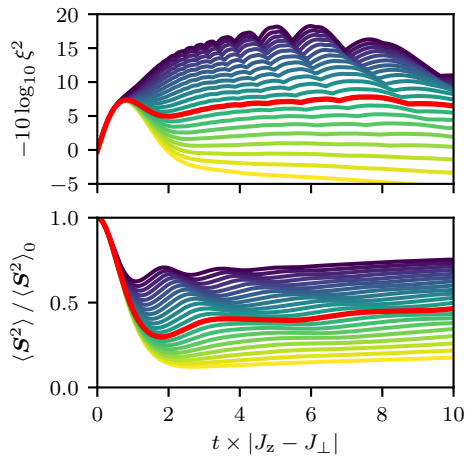


FIG. 3. Squeezing  $\xi^2$  (top) and squared spin length  $\langle \mathbf{S}^2 \rangle$  (bottom) over time for the power-law XXZ model with  $\alpha = 3$  and  $J_z/J_\perp$  ranging from  $-1$  (blue) to  $-3$  (yellow) on a 2D lattice of  $64 \times 64$  spins. The red lines marks the approximate transition ( $J_z/J_\perp = -2.2$ ) at which the “collective” squeezing peak at  $\tau \equiv t \times |J_z - J_\perp| \sim 6$  drops below the “Ising” peak at  $\tau \sim 1$ . For the parameters shown,  $\langle \mathbf{S}^2 \rangle$  reaches a minimum at  $\tau \sim 2$ , which means that optimal squeezing at  $\tau \sim 1$  is reached before maximal decay of  $\langle \mathbf{S}^2 \rangle$  in the “Ising” phase.

thus deserves further study in future work.

It is no surprise that quantities such as  $t_{\text{opt}}$  and  $\langle \mathbf{S}^2 \rangle_{\text{min}}$  that are defined via minimization exhibit discontinuous behavior, and these discontinuities do not by themselves indicate a transition between different phases of matter. We can formally distinguish between the dynamical phases of collective and Ising-limited squeezing behavior seen in Figure 2 by examining the nature of squeezing and entanglement that is generated within each phase. Specifically, the Ising-limited phase generates an amount of entanglement that is insensitive to system size, whereas the collective phase generates an amount of squeezing that grows with system size (see Figure 4). This growth is well described by a power-law  $\xi_{\text{opt}}^2 \sim 1/N^\nu$  with an exponent  $\nu$  that depends on the values of  $\alpha$  and  $J_z/J_\perp$  (see [35]). Numerically, we find that the transition between collective and Ising-limited dynamical phases occurs at a critical ZZ coupling  $J_z^{\text{crit}}$  that diverges logarithmically with system size,  $J_z^{\text{crit}} \sim -J_\perp \log N$  [35]. In contrast to the discontinuities of  $t_{\text{opt}}$  and  $\langle \mathbf{S}^2 \rangle_{\text{min}}$  at the dynamical phase boundary, discontinuities in these quantities *within* the collective phase (see Figure 2) can be attributed to the presence of small oscillations in squeezing over time (see Figure 3). We assign no particular significance to the competition between squeezing peaks associated with these oscillations, but note that these oscillations add minor corrections to the collective-phase scaling  $\xi_{\text{opt}}^2 \sim 1/N^\nu$  and  $J_z^{\text{crit}} \sim -J_\perp \log N$  in Figure 4.

Though primarily used as a measure of metrological utility, the squeezing parameter  $\xi^2$  is also a witness of

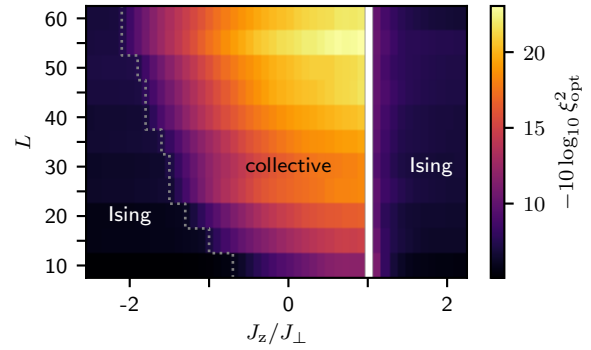


FIG. 4. Optimal squeezing  $\xi_{\text{opt}}^2$  as a function of system size for the power-law XXZ model with  $\alpha = 3$  on a 2D lattice of  $N = L \times L$  spins. Whereas the amount of squeezing generated in the Ising dynamical phase is insensitive to system size, collective dynamics generate squeezing that grows with system size and as  $J_z/J_\perp \rightarrow 1$  (from below), resulting in a system size-dependent boundary between dynamical phases. Dotted grey line tracks minima of  $\langle \mathbf{S}^2 \rangle_{\text{min}}$  as a function of  $J_z/J_\perp$ , as in Figure 2, marking the approximate dynamical phase boundary.

many-body entanglement that can be detected by the means and variances of collective spin observables (linear combinations of  $S_x, S_y, S_z$ ) [24, 25]. Squeezing that scales as  $\xi^2 \sim 1/N^\nu$  implies an *entanglement depth*  $k \sim N^\nu$ , which quantifies the minimum number of mutually entangled particles in a given state [24, 44]. The XXZ model is thus an interesting case for the study of large-scale entanglement growth in short-range interacting systems.

*Experimental applications* – As indicated in Figure 2, our results are readily applicable to the generation of spin squeezed states in a variety of experimental platforms that have been shown to implement the XXZ model with different  $\alpha$ , including neutral atoms ( $\alpha \rightarrow \infty$ ) [40, 41], Rydberg atoms ( $\alpha = 3, 6$ ) [28, 29, 42], polar molecules ( $\alpha = 3$ ) [30, 31, 43], and magnetic atoms ( $\alpha = 3$ ) [32, 33]. Note that one may additionally have to consider the effects of a sub-unit filling fraction on the realization of a spin model. In principle, sub-unit filling introduces effective disorder into the XXZ spin couplings [22, 45]. Nonetheless, the precise form of these interactions is not essential to the existence of a collective dynamical phase in the XXZ model, as evidenced by the fact that this phase persists through to the  $\alpha \rightarrow \infty$  limit of nearest-neighbor interactions (see also [35]).

Finally, we discuss the application of our results to Ising systems without 3D spin-aligning  $\mathbf{s}_i \cdot \mathbf{s}_j$  interactions, as in the case of some Rydberg atom ( $\alpha = 3, 6$ ) [28, 29] and trapped ion ( $0 \leq \alpha < 3$ ) [11] experiments. In this case, 2D spin-aligning interactions within the  $y$ - $z$  plane can still be engineered by the application of a strong transverse driving field  $\Omega S_x$ . If the drive strength  $\Omega \gg \frac{1}{2} N h_\alpha J_z$ , with  $h_\alpha$  the mean of  $1/|\mathbf{r}_i - \mathbf{r}_j|^\alpha$  over all  $i \neq j$ , then moving into the rotating frame of the drive

and eliminating fast-oscillating terms results in an XX model described by the Hamiltonian

$$H_{\text{XX}} = \frac{J_z}{2} \sum_{i \neq j} \frac{s_{y,i}s_{y,j} + s_{z,i}s_{z,j}}{|\mathbf{r}_i - \mathbf{r}_j|^\alpha}, \quad (4)$$

which is a special case of the XXZ model in Eq. (3), with  $(J_\perp, J_z) \rightarrow (J_z/2, 0)$ . Ising systems with a strong transverse field can thus access a vertical cut along  $J_z = 0$  in Figure 2.

*Conclusion* – We have used DTWA to study the spin squeezing behavior of the XXZ model with power-law interactions that fall off with distance  $r$  as  $1/r^\alpha$  in  $D = 2$  and 3 spatial dimensions. Surprisingly, we have found that squeezing comparable to the infinite-range OAT limit ( $\alpha = 0$ ) can still be achievable with short-range interactions, when  $\alpha > D$ . A collective dynamical phase in which attainable squeezing and entanglement depth scale with system size extends all the way through to the  $\alpha \rightarrow \infty$  limit of nearest-neighbor interactions. Our findings are readily applicable to metrological efforts with a variety of cold atomic, molecular, and optical platforms.

*Acknowledgments* – We thank Sean R. Muleady and Jeremy T. Young for reviewing this manuscript. This work is supported by the DARPA DRINQs grant, the ARO single investigator award W911NF-19-1-0210, NSF grant PHY-1820885, AFOSR grant FA9550-19-1-0275, NSF grant PHY-1734006 (JILA-PFC), and by NIST.

and J. Ye, A Quantum Many-Body Spin System in an Optical Lattice Clock, *Science* **341**, 632 (2013).

- [10] P. He, M. A. Perlin, S. R. Muleady, R. J. Lewis-Swan, R. B. Hutson, J. Ye, and A. M. Rey, Engineering spin squeezing in a 3D optical lattice with interacting spin-orbit-coupled fermions, *Physical Review Research* **1**, 033075 (2019).
- [11] J. W. Britton, B. C. Sawyer, A. C. Keith, C.-C. J. Wang, J. K. Freericks, H. Uys, M. J. Biercuk, and J. J. Bollinger, Engineered two-dimensional Ising interactions in a trapped-ion quantum simulator with hundreds of spins, *Nature* **484**, 489 (2012).
- [12] J. G. Bohnet, B. C. Sawyer, J. W. Britton, M. L. Wall, A. M. Rey, M. Foss-Feig, and J. J. Bollinger, Quantum spin dynamics and entanglement generation with hundreds of trapped ions, *Science* **352**, 1297 (2016).
- [13] K. Baumann, C. Guerlin, F. Brennecke, and T. Esslinger, Dicke quantum phase transition with a superfluid gas in an optical cavity, *Nature* **464**, 1301 (2010).
- [14] H. Ritsch, P. Domokos, F. Brennecke, and T. Esslinger, Cold atoms in cavity-generated dynamical optical potentials, *Reviews of Modern Physics* **85**, 553 (2013).
- [15] M. A. Norcia, R. J. Lewis-Swan, J. R. K. Cline, B. Zhu, A. M. Rey, and J. K. Thompson, Cavity-mediated collective spin-exchange interactions in a strontium super-radiant laser, *Science* **361**, 259 (2018).
- [16] R. M. Kroeze, Y. Guo, V. D. Vaidya, J. Keeling, and B. L. Lev, Spinor Self-Ordering of a Quantum Gas in a Cavity, *Physical Review Letters* **121**, 163601 (2018).
- [17] E. J. Davis, G. Bentsen, L. Homeier, T. Li, and M. H. Schleier-Smith, Photon-Mediated Spin-Exchange Dynamics of Spin-1 Atoms, *Physical Review Letters* **122**, 010405 (2019).
- [18] M. Foss-Feig, Z.-X. Gong, A. V. Gorshkov, and C. W. Clark, Entanglement and spin-squeezing without infinite-range interactions, arXiv:1612.07805 [cond-mat, physics:quant-ph] (2016).
- [19] A. M. Rey, L. Jiang, M. Fleischhauer, E. Demler, and M. D. Lukin, Many-body protected entanglement generation in interacting spin systems, *Physical Review A* **77**, 052305 (2008).
- [20] P. Cappellaro and M. D. Lukin, Quantum correlation in disordered spin systems: Applications to magnetic sensing, *Physical Review A* **80**, 032311 (2009).
- [21] M. P. Kwasigroch and N. R. Cooper, Bose-Einstein condensation and many-body localization of rotational excitations of polar molecules following a microwave pulse, *Physical Review A* **90**, 021605 (2014).
- [22] M. P. Kwasigroch and N. R. Cooper, Synchronization transition in dipole-coupled two-level systems with positional disorder, *Physical Review A* **96**, 053610 (2017).
- [23] E. J. Davis, A. Periwal, E. S. Cooper, G. Bentsen, S. J. Evered, K. Van Kirk, and M. H. Schleier-Smith, Protecting Spin Coherence in a Tunable Heisenberg Model, arXiv:2003.06087 [cond-mat, physics:quant-ph] (2020).
- [24] A. S. Sørensen and K. Mølmer, Entanglement and Extreme Spin Squeezing, *Physical Review Letters* **86**, 4431 (2001).
- [25] G. Tóth, C. Knapp, O. Gühne, and H. J. Briegel, Optimal Spin Squeezing Inequalities Detect Bound Entanglement in Spin Models, *Physical Review Letters* **99**, 250405 (2007).
- [26] M. A. Cazalilla and A. M. Rey, Ultracold fermi gases with emergent  $SU(n)$  symmetry, *Reports on Progress in Physics* **82**, 076001 (2019).

\* [mika.perlin@gmail.com](mailto:mika.perlin@gmail.com)

† Authors M.A.P. and C.Q. contributed equally to this work.

- [1] V. Giovannetti, S. Lloyd, and L. Maccone, Quantum Metrology, *Physical Review Letters* **96**, 010401 (2006).
- [2] V. Giovannetti, S. Lloyd, and L. Maccone, Advances in quantum metrology, *Nature Photonics* **5**, 222 (2011).
- [3] G. Tóth and I. Apellaniz, Quantum metrology from a quantum information science perspective, *Journal of Physics A: Mathematical and Theoretical* **47**, 424006 (2014).
- [4] M. Szczykulska, T. Baumgratz, and A. Datta, Multi-parameter quantum metrology, *Advances in Physics: X* **1**, 621 (2016).
- [5] D. J. Wineland, J. J. Bollinger, W. M. Itano, F. L. Moore, and D. J. Heinzen, Spin squeezing and reduced quantum noise in spectroscopy, *Physical Review A* **46**, R6797 (1992).
- [6] J. Ma, X. Wang, C. P. Sun, and F. Nori, Quantum spin squeezing, *Physics Reports* **509**, 89 (2011).
- [7] M. Kitagawa and M. Ueda, Squeezed spin states, *Physical Review A* **47**, 5138 (1993).
- [8] T. Zibold, E. Nicklas, C. Gross, and M. K. Oberthaler, Classical Bifurcation at the Transition from Rabi to Josephson Dynamics, *Physical Review Letters* **105**, 204101 (2010).
- [9] M. J. Martin, M. Bishof, M. D. Swallows, X. Zhang, C. Benko, J. von-Stecher, A. V. Gorshkov, A. M. Rey,

Physics **77**, 124401 (2014).

[27] C. Gross and I. Bloch, Quantum simulations with ultracold atoms in optical lattices, *Science* **357**, 995 (2017).

[28] C. S. Adams, J. D. Pritchard, and J. P. Shaffer, Rydberg atom quantum technologies, *Journal of Physics B: Atomic, Molecular and Optical Physics* **53**, 012002 (2019).

[29] A. Browaeys and T. Lahaye, Many-body physics with individually controlled Rydberg atoms, *Nature Physics* **16**, 132 (2020).

[30] J. L. Bohn, A. M. Rey, and J. Ye, Cold molecules: Progress in quantum engineering of chemistry and quantum matter, *Science* **357**, 1002 (2017).

[31] S. A. Moses, J. P. Covey, M. T. Miecnikowski, D. S. Jin, and J. Ye, New frontiers for quantum gases of polar molecules, *Nature Physics* **13**, 13 (2017).

[32] S. Lepoutre, J. Schachenmayer, L. Gabardos, B. Zhu, B. Naylor, E. Maréchal, O. Gorceix, A. M. Rey, L. Vernac, and B. Laburthe-Tolra, Out-of-equilibrium quantum magnetism and thermalization in a spin-3 many-body dipolar lattice system, *Nature Communications* **10**, 1714 (2019).

[33] A. Patscheider, B. Zhu, L. Chomaz, D. Petter, S. Baier, A.-M. Rey, F. Ferlaino, and M. J. Mark, Controlling dipolar exchange interactions in a dense three-dimensional array of large-spin fermions, *Physical Review Research* **2**, 023050 (2020).

[34] C. D. Bruzewicz, J. Chiaverini, R. McConnell, and J. M. Sage, Trapped-ion quantum computing: Progress and challenges, *Applied Physics Reviews* **6**, 021314 (2019).

[35] see supplementary material.

[36] M. Foss-Feig, K. R. A. Hazzard, J. J. Bollinger, and A. M. Rey, Nonequilibrium dynamics of arbitrary-range Ising models with decoherence: An exact analytic solution, *Physical Review A* **87**, 042101 (2013).

[37] M. van den Worm, B. C. Sawyer, J. J. Bollinger, and M. Kastner, Relaxation timescales and decay of correlations in a long-range interacting quantum simulator, *New Journal of Physics* **15**, 083007 (2013).

[38] J. Schachenmayer, A. Pikovski, and A. M. Rey, Many-Body Quantum Spin Dynamics with Monte Carlo Trajectories on a Discrete Phase Space, *Physical Review X* **5**, 011022 (2015).

[39] J. Schachenmayer, A. Pikovski, and A. M. Rey, Dynamics of correlations in two-dimensional quantum spin models with long-range interactions: A phase-space Monte-Carlo study, *New Journal of Physics* **17**, 065009 (2015).

[40] L.-M. Duan, E. Demler, and M. D. Lukin, Controlling Spin Exchange Interactions of Ultracold Atoms in Optical Lattices, *Physical Review Letters* **91**, 090402 (2003).

[41] Y.-A. Chen, S. Nascimbène, M. Aidelsburger, M. Atala, S. Trotzky, and I. Bloch, Controlling Correlated Tunneling and Superexchange Interactions with ac-Driven Optical Lattices, *Physical Review Letters* **107**, 210405 (2011).

[42] A. Signoles, T. Franz, R. F. Alves, M. Gärttner, S. Whitlock, G. Zürn, and M. Weidmüller, Glassy dynamics in a disordered Heisenberg quantum spin system, arXiv:1909.11959 [cond-mat, physics:physics, physics:quant-ph] (2020).

[43] A. V. Gorshkov, S. R. Manmana, G. Chen, J. Ye, E. Demler, M. D. Lukin, and A. M. Rey, Tunable Superfluidity and Quantum Magnetism with Ultracold Polar Molecules, *Physical Review Letters* **107**, 115301 (2011).

[44] G. Vitagliano, I. Apellaniz, M. Kleinmann, B. Lücke, C. Klempert, and G. Tóth, Entanglement and extreme spin squeezing of unpolarized states, *New Journal of Physics* **19**, 013027 (2017).

[45] K. R. A. Hazzard, S. R. Manmana, M. Foss-Feig, and A. M. Rey, Far-from-Equilibrium Quantum Magnetism with Ultracold Polar Molecules, *Physical Review Letters* **110**, 075301 (2013).

### Spectral gap of the long-range critical XXZ model

Here we show that the critical ( $J_z = J_{\perp}$ ) XXZ model in Eq. (3) has a spectral gap when  $\alpha \leq D$ , which implies the existence of a finite range of ZZ couplings  $J_z \approx J_{\perp}$  for which the XXZ model formally recovers the OAT model at first order in perturbation theory. For definiteness, we consider a critical XXZ model on a cubic lattice with periodic boundary conditions in  $D$  dimensions. The translational and  $SU(2)$  symmetries of the critical XXZ model on such a lattice imply that its lowest-lying excitations can be written as spin waves of the form

$$|m_z, k\rangle \propto \sum_{n \in \mathbb{Z}_L^D} e^{ik \cdot n} s_{z,n} |m_z\rangle, \quad (5)$$

where  $|m_z\rangle$  is a permutationally-symmetric Dicke state with spin projection  $m_z$  onto the  $z$  axis,  $n = (n_1, n_2, \dots, n_D)$  indexes an individual site on the lattice of  $N = L^D$  spins, and  $k \in \mathbb{Z}_L^D \times 2\pi/L$  is a wavenumber. The energy of the state  $|m_z, k\rangle$  with respect to the critical XXZ Hamiltonian is

$$E_k = -J_{\perp} \sum_{\substack{n \in \mathbb{Z}_L^D \\ |n| \neq 0}} \frac{1 - \cos(k \cdot n)}{|n|^{\alpha}}, \quad (6)$$

where for simplicity we work in units for which the lattice spacing is 1. The energy  $E_k$  is minimized (in magnitude) by a wavenumber that undergoes one oscillation across one axis of the lattice, e.g.  $k = (2\pi/L, 0, 0, \dots)$ , which implies

a spectral gap

$$\Delta_{\text{gap}} = |J_{\perp}| \sum_{\substack{n \in \mathbb{Z}_L^D \\ |n| \neq 0}} \frac{1 - \cos(2\pi n_1)}{|n|^{\alpha}}. \quad (7)$$

Letting  $\epsilon \equiv 2/L$ , we define a rescaled domain  $\mathbb{S}_{\epsilon} = \mathbb{Z}_L/\epsilon \subset [-1, 1]$ , and substitute  $x = \epsilon n$  to get

$$\Delta_{\text{gap}} = |J_{\perp}| \epsilon^{\alpha-D} \sum_{\substack{x \in \mathbb{S}_{\epsilon}^D \\ |x| \geq \epsilon}} \epsilon^D \frac{1 - \cos(\pi x_1)}{|x|^{\alpha}}, \quad (8)$$

which in the thermodynamic limit  $\epsilon \rightarrow 0$  is well approximated by an integral that avoids an infinitesimal region at the origin,

$$\Delta_{\text{gap}} \rightarrow |J_{\perp}| \epsilon^{\alpha-D} \mathcal{I}_D(\epsilon), \quad \mathcal{I}_D(\epsilon) \equiv \int_{\mathbb{T}_1^D \setminus \mathbb{T}_{\epsilon}^D} d^D x \frac{1 - \cos(\pi x_1)}{|x|^{\alpha}}, \quad (9)$$

where  $\mathbb{T}_a \equiv (-a, a)$  is a symmetric interval about 0. The integrand of  $\mathcal{I}_D(\epsilon)$  is strictly positive and well-behaved on the entirety of its domain except for the origin, where depending on the value of  $\alpha$  the integrand may vanish or diverge as  $|x| \rightarrow 0$ . Together, these facts mean that

$$\mathcal{I}_D(\epsilon) \xrightarrow{\epsilon \rightarrow 0} \epsilon^{-\gamma}, \quad \Delta_{\text{gap}} \xrightarrow{\epsilon \rightarrow 0} \epsilon^{\alpha-D-\gamma}, \quad (10)$$

for some  $\gamma > 0$ , which implies that  $\Delta_{\text{gap}} > 0$  when  $\alpha \leq D \leq D + \gamma$ .

### Numerical results in one spatial dimension

Here we provide additional DTWA simulation results for the squeezing behavior of the power-law XXZ model in  $D = 1$  spatial dimension. Figure 5 shows results analogous to those in Figure 2 of the main text, for  $D = 1, 2, 3$  spatial dimensions and integer values of the power-law exponent  $\alpha$  (as well as the  $\alpha \rightarrow \infty$  limit of nearest-neighbor interactions). The existence of a collective dynamical phase persists in one spatial dimension, but for a much narrower range of parameters than in the case of  $D = 2$  and 3. The achievable squeezing in the collective phase also scales less favorably with system size in the case of  $D = 1$ . Nonetheless, squeezing beyond the Ising limit is still achievable in  $D = 1$  with  $J_z = 0$  and  $\alpha > 1$ , which is relevant for trapped ion experiments.

### Benchmarking DTWA for the XXZ model

In order to gauge the reliability of DTWA for the XXZ model in this work, we benchmark against *truncated shell* (TS<sub>4</sub>) simulations of a  $7 \times 7$  spin lattice whose dynamics are restricted to the subspace of  $\sim N^5$  states with definite total spin  $S \geq N/2 - 4$ . These simulations are motivated by the idea that spin-aligning  $\mathbf{s}_i \cdot \mathbf{s}_j$  interactions energetically suppress the decay of total spin  $S$  from its initial value of  $N/2$  in a spin-polarized state. As long as the total spin decay is small, TS<sub>4</sub> simulations should faithfully capture the dynamical behavior of a system. The advantage of TS<sub>4</sub> simulations over DTWA is that TS<sub>4</sub> is “self-benchmarking,” in the sense that its breakdown can be diagnosed by a large population of the  $S = N/2 - 4$  manifold, which indicates further population leakage into truncated states with  $S < N/2 - 4$  (see Figure 6).

We benchmark DTWA simulations against TS<sub>4</sub> in Figure 7 by comparing two observables of interest: (i) the optimal spin squeezing parameter  $\xi_{\text{opt}}^2 \equiv \min_t \xi^2(t) = \xi^2(t_{\text{opt}})$ , and the minimal value of  $\langle \mathbf{S}^2 \rangle$  throughout squeezing dynamics,  $\langle \mathbf{S}^2 \rangle_{\text{min}} \equiv \min_{t \leq t_{\text{opt}}} \langle \mathbf{S}^2 \rangle(t)$ . For reference, Figure 7 also shows the values of  $\xi_{\text{opt}}^2$  and  $\langle \mathbf{S}^2 \rangle_{\text{min}}$  in the exactly solvable limits of uniform (OAT,  $\alpha = 0$ ) and power-law Ising ( $J_{\perp} = 0$ ) interactions. For initially spin-polarized states, these limits have only one relevant energy scale,  $J_z - J_{\perp}$ , so the only effect of changing  $J_z$  is to change dynamical time scales.

The results in Figure 7 show that DTWA agrees almost exactly with TS<sub>4</sub> in the regimes that TS<sub>4</sub> can be trusted, suggesting that DTWA is a reliable method for studying the spin squeezing behavior of the XXZ model. Values of squeezing  $-10 \log_{10} \xi^2 > 0$  are highly sensitive to errors in collective spin observables, so more pronounced (albeit

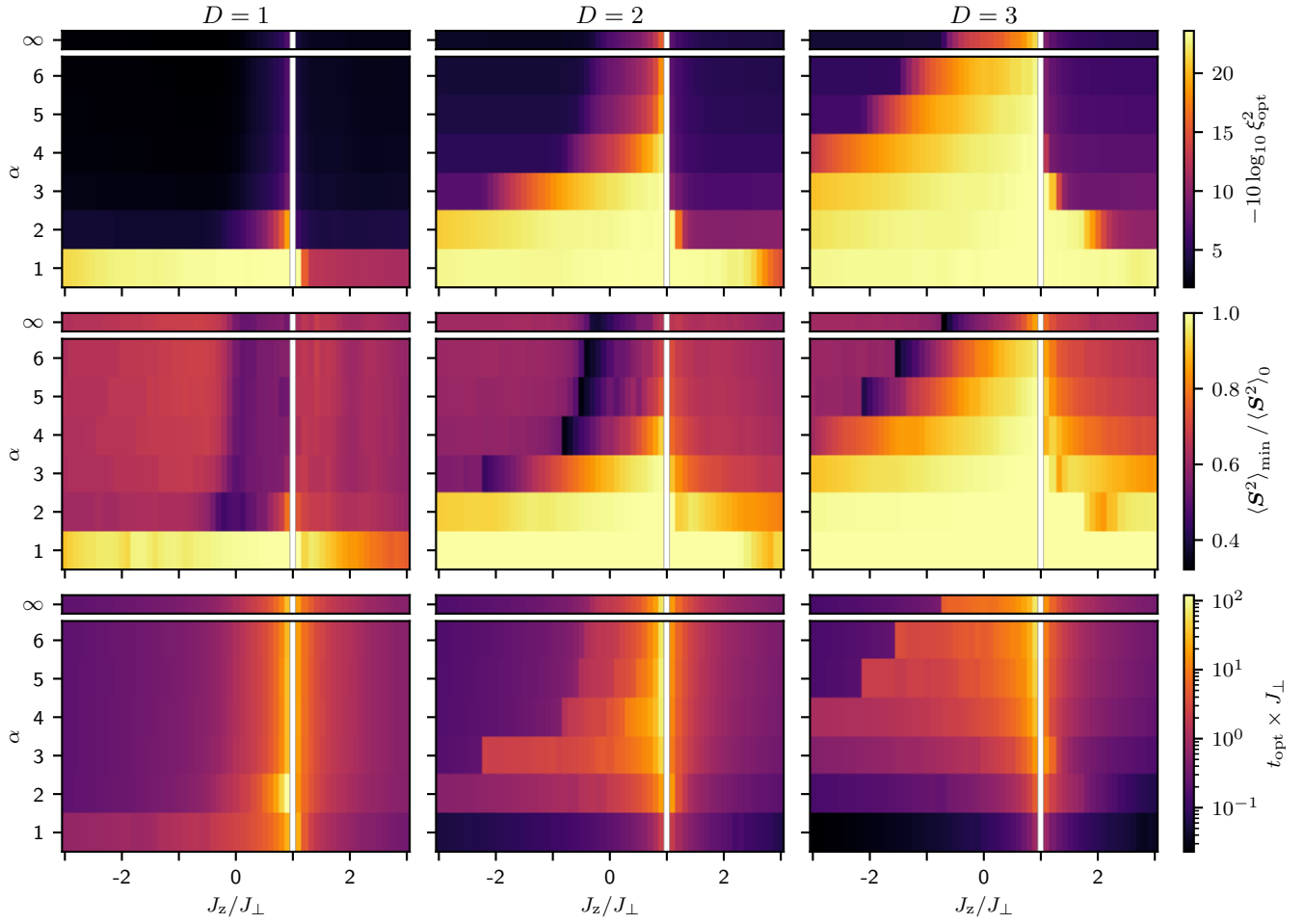


FIG. 5. The optimal squeezing  $\xi_{\text{opt}}^2$  (top), minimal squared spin length  $\langle \mathbf{S}^2 \rangle_{\text{min}}$  (middle), and optimal squeezing time  $t_{\text{opt}}$  (bottom) for  $4096 = 64^2 = 16^3$  spins in  $D = 1, 2, 3$  spatial dimensions. Spins are initially polarized along the equator and evolved under the XXZ Hamiltonian in Eq. (3). The results for  $D = 2$  and  $3$  shown here are a subset of the results in Figure 2, presented in the same format as that for  $D = 1$  for the sake of comparison.

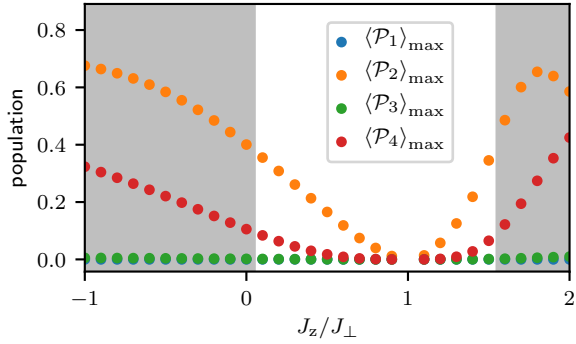


FIG. 6. Maximal populations  $\langle \mathcal{P}_n \rangle_{\text{max}}$  of the total spin  $S = N/2 - n$  manifolds  $\mathcal{P}_n$  throughout squeezing dynamics of  $7 \times 7$  spins, initially polarized along the equator and evolved under the XXZ Hamiltonian in Eq. (3) with a power-law exponent  $\alpha = 3$ . Computed with TS<sub>4</sub> simulations and periodic boundary conditions. Shaded regions indicate  $\langle \mathcal{P}_4 \rangle_{\text{max}} > 0.1$ , where TS<sub>4</sub> results cannot be trusted due to the likeliness of population leakage into truncated states. All states in  $\mathcal{P}_1$  break translational invariance, so the initial population  $\langle \mathcal{P}_1 \rangle_0 = 0$  is protected by the absence of translational symmetry-breaking terms in the Hamiltonian. The population  $\langle \mathcal{P}_3 \rangle$ , meanwhile, is small because  $\mathcal{P}_3$  is only coupled to  $\mathcal{P}_2$  and  $\mathcal{P}_4$  by matrix elements that are  $O(1/N)$  smaller than the couplings between  $\mathcal{P}_0 \leftrightarrow \mathcal{P}_2 \leftrightarrow \mathcal{P}_4$ .

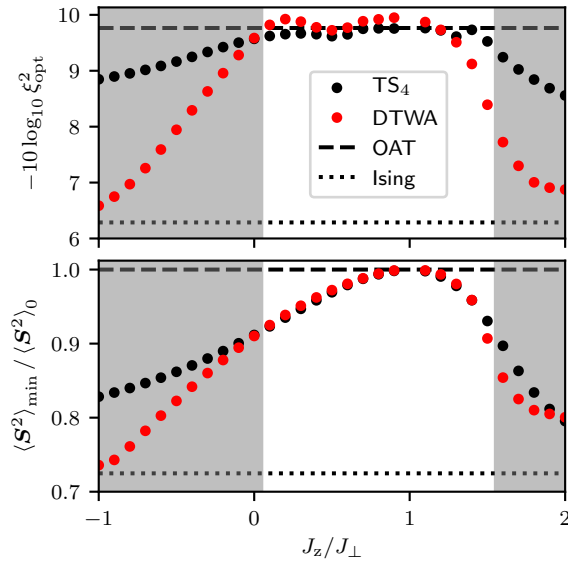


FIG. 7. Optimal squeezing  $\xi_{\text{opt}}^2$  (top) and minimal squared spin length  $\langle \mathbf{S}^2 \rangle_{\text{min}}$  throughout squeezing dynamics (bottom) as computed via  $\text{TS}_4$  and DTWA in the same setting as Figure 6, likewise with shaded regions indicating  $\langle \mathcal{P}_4 \rangle_{\text{max}} > 0.1$  in the  $\text{TS}_4$  simulations. Here squeezing  $\xi_{\text{opt}}^2$  is shown in decibels, with  $-\log \xi_{\text{opt}}^2 > 0$ , and  $\langle \mathbf{S}^2 \rangle_{\text{min}}$  is normalized to its initial value  $\langle \mathbf{S}^2 \rangle_0 = \frac{N}{2} \left( \frac{N}{2} + 1 \right)$ . Dashed and dotted lines respectively mark the exactly solvable limits of uniform (OAT,  $\alpha = 0$ ) and power-law Ising ( $J_{\perp} = 0$ ) interactions.

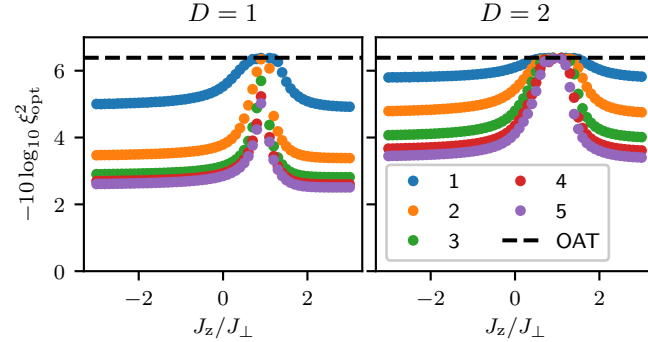


FIG. 8. Optimal squeezing  $\xi_{\text{opt}}^2$  as a function of  $J_z/J_{\perp}$  on a lattice of  $16 = 4 \times 4$  spins in  $D = 1$  and 2 spatial dimensions, computed using exact methods. The color of each marker indicates the corresponding value of  $\alpha$ , as specified in the legend, and the dashed line marks the OAT limit of  $\alpha = 0$ .

minor) disagreements in spin squeezing between DTWA and  $\text{TS}_4$  are expected. Also, for the sake of clarity we used a simple heuristic to identify regimes of validity for  $\text{TS}_4$  in Figures 6 and 7. This heuristic is not intended to be a precise indicator of quantitative accuracy for  $\text{TS}_4$ , so it is no surprise that it does not identify the precise values of  $J_z$  at which DTWA and  $\text{TS}_4$  diverge.

Finally, we provide exact results for the optimal squeezing parameter  $\xi_{\text{opt}}^2$  on a lattice of  $16 = 4 \times 4$  spins in  $D = 1$  and 2 spatial dimensions, in Figure 8. Though optimal squeezing saturates to a finite-size value fairly quickly away from the critical point at  $J_z = J_{\perp}$ , a collective region with OAT-limited squeezing still appears when  $J_z \approx J_{\perp}$ .

### Scaling relations for the collective dynamical phase

Here we inspect the results in Figure 4 of the main text in more detail to show that (i) optimal squeezing scales as  $\xi_{\text{opt}}^2 \sim 1/N^{\nu}$  in the collective dynamical phase (Figure 9), and (ii) the critical ZZ coupling  $J_z^{\text{crit}}$  at the collective-to-Ising dynamical phase boundary diverges logarithmically with system size,  $J_z^{\text{crit}} \sim -J_{\perp} \log N$  (Figure 10). Note that the exponent  $\nu$  will generally depend on the values of  $J_z/J_{\perp}$  and  $\alpha$ , and that the exact coefficient in the logarithmic

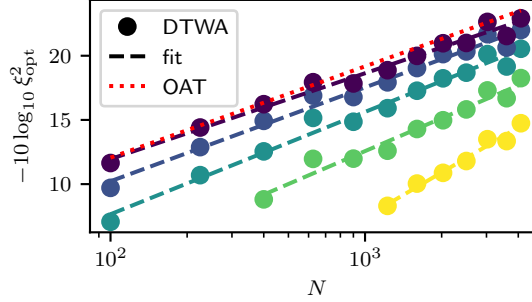


FIG. 9. Dependence of the optimal squeezing parameter  $\xi_{\text{opt}}^2$  on system size  $N$  within the collective dynamical phase of the XXZ model in Eq. (3) with power-law exponent  $\alpha = 3$  in  $D = 2$  spatial dimensions. Color indicates the value of  $J_z/J_{\perp}$ , ranging from  $-1.5$  (yellow, bottom) to  $+0.5$  (purple, top) in increments of  $0.5$ . Circles show results computed with DTWA; dashed lines show a fit to  $\xi_{\text{opt}}^2 = a/N^{\nu}$  with free parameters  $a, \nu$ ; and the dotted red line marks the OAT limit for reference. The DTWA results in this figure are a subset of those in Figure 4 of the main text.

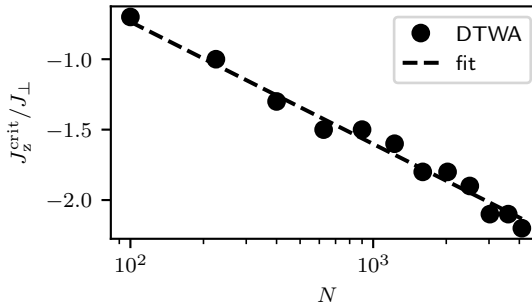


FIG. 10. Dependence of the critical ZZ coupling  $J_z^{\text{crit}}$  at the collective-to-Ising dynamical phase boundary on system size  $N$  for the XXZ model in Eq. (3) with power-law exponent  $\alpha = 3$  in  $D = 2$  spatial dimensions. Circles show results computed with DTWA (same as the dotted grey lines in Figure 4 of the main text), and the dashed line shows a fit to  $J_z^{\text{crit}}/J_{\perp} - 1 = b \ln N$ .

dependence of  $J_z^{\text{crit}}$  on  $N$  will similarly depend on the value of  $\alpha$ . Small oscillations in squeezing over time, seen in Figure 3 of the main text, add minor corrections to the collective-phase scaling  $\xi_{\text{opt}}^2 \sim 1/N^{\nu}$  and  $J_z^{\text{crit}} \sim -J_{\perp} \log N$ . Some deviation is also attributed to the approximations made by DTWA. Numerically, we find that  $\xi_{\text{opt}}^2 \approx a/N^{\nu}$  with  $\nu \approx (1.16, 0.85, 0.80, 0.73, 0.67)$  for  $J_z/J_{\perp} = (-1.5, -1, -0.5, 0, 0.5)$ , and  $J_z^{\text{crit}}/J_{\perp} - 1 \approx -b \ln N$  for  $b = 0.377 \pm 0.002$  on a 2-dimensional square lattice with  $\alpha = 3$ . The fact that  $\nu > 2/3$  (and, in particular,  $\nu > 1$  for  $J_z/J_{\perp} = -1.5$ ) suggests that optimal squeezing parameter  $\xi_{\text{opt}}^2$  eventually saturates to a different scaling law with a smaller exponent ( $\nu$ ) at sufficiently large system sizes ( $N$ ).

### Sub-unit filling fractions

Though we do not study the effect of variable filling fractions in detail, here we show that the collective phase is stable to filling fractions  $f < 1$ . To this end, in Figure 11 we show the dependence of the optimal squeezing parameter  $\xi_{\text{opt}}^2$  on filling fraction  $f$  on a  $50 \times 50$  lattice in  $D = 2$  two spatial dimensions with power-law exponent  $\alpha = 3$  (as in the case of polar molecules, for which unit filling is difficult to obtain experimentally). Optimal squeezing generally decreases with filling fraction, which is in part attributable to a changing particle number. Nonetheless, squeezing well in excess of the Ising limit is clearly achievable even for small filling fractions,  $f \sim 0.1$ , as long as the XXZ model is tuned sufficiently close to the critical point at  $J_z = J_{\perp}$ .

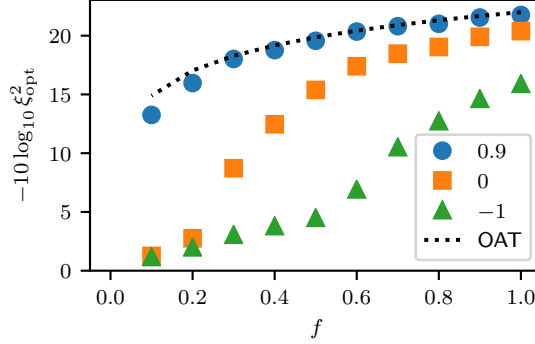


FIG. 11. Dependence of the optimal squeezing parameter  $\xi_{\text{opt}}^2$  on filling fraction  $f$  for the XXZ model in Eq. (3) with power-law exponent  $\alpha = 3$  in  $D = 2$  spatial dimensions with  $50 \times 50$  lattice sites. Results computed using DTWA, with a random choice of  $f \times 50 \times 50$  lattice sites to occupy. The shape and color of each marker indicates the corresponding value of  $J_z/J_{\perp}$ , as specified in the legend, and the dotted line marks the OAT limit for reference.